ELSEVIER

Ceramics International 33 (2007) 155–161

CERAMICS INTERNATIONAL

www.elsevier.com/locate/ceramint

Synthesis and characterization of WC–Co nanocomposites by novel chemical method

M.F. Zawrah *

Ceramics Department, National Research Center, 12622 Dokki, Cairo, Egypt

Received 17 May 2005; received in revised form 28 July 2005; accepted 7 September 2005
Available online 18 January 2006

Abstract

Nanocrystalline WC–Co cemented carbides containing different proportions of cobalt, i.e. 5, 10 and 15 wt.%, were prepared by chemical route. Another series of these composites containing 10 wt.% of cobalt with 5 wt.% Fe or Mn or Zn or Ni were also prepared by the same method. Polyacrylonitrile and tungestic acid were used as a source of carbon and tungsten, respectively. Phase composition, crystallite sizes and microstructure evaluation were investigated by X-ray diffraction (XRD), transmission electron microscope (TEM) and scanning electron microscope (SEM). The results revealed that the present chemical method is effective route to synthesize nanocrystalline WC–Co composites. By doping Co and/or Fe or Mn or Zn or Ni in WC–Co nanocomposite, nanocrystalline cemented carbide with inhibited grain growth were obtained. XRD showed peaks characterizing WC and Co in case of WC–15 wt.% Co, but showed addition peaks characterizing some oxides of tungsten and cobalt with W metal in case of WC–10 wt.% Co and/or 5 wt.% Fe of Mn or Zn or Ni. The crystallite size of the prepared WC–15 wt.% Co and heat-treated at 1000 °C was in the range of 1.1–7.4 nm, while it was 12–50 nm for WC–Co containing Fe or Mn or Zn or Ni as detected from XRD. On the other hand, the particle size was in the range of 200–400 and 300–500 nm, respectively, as detected from TEM and SEM.

Keywords: Nanomaterial; WC–Co; Ceramics

1. Introduction

Research in nanostructured materials has been extremely active over the past two decades. While considerable properties advantages of nanostructured materials over conventional coarse-grained counterparts have been demonstrated in laboratories, the shift from laboratory experiments to technological applications has been slow [1]. WC–Co cemented carbides are today an integrated component of many industrial operations including military, aerospace, automotive, electronics, mining, grinding and metal cutting. Their widespread application results from the composite physical and mechanical properties of abrasive-wear resistance, chemical-wear resistance, high hardness and toughness. The mechanical properties are strongly dependant on the microstructure, e.g. the hardness increases with increase carbide grain size [2–5]. Although refractory ceramic materials such as WC, TiC and SiC satisfy several of these requirements, the low toughness of ceramics causes brittle fracture. This difficulty has been overcome to some extent by addition of ductile metal to give ceramic–metal composites. But, the addition of a large amount of metal will reduce the hardness. The toughness of the ceramics can, however, be increased remarkably without sacrificing the hardness by reducing the grain size [6]. Composite systems in which the components have nanometer size (nanocomposites) offer significantly better mechanical properties than those with micrometer-size components [7,8]. The large surface and grain boundary energies associated with the nanocomposites also provide enhanced driving force for densification.

The current industrial process for manufacturing conventional (i.e. coarse-grained) WC–Co powders involves production of WC and Co separately, and forming the cement powder by mixing the two constituents [2–5]. Specifically, it requires at least five steps, i.e. step 1: tungsten powders is produced from hydrogen reduction of chemically purified tungsten oxide (WO_3) at 700–900 °C for about 5 h; step 2: W powder is carbonized by mixing with carbon black through milling for 6–8 h, followed by heating in hydrogen at 1400–1600 °C for 10 h; step 3: WC blacks produced from step 2 is crushed in a hammer mill, ground in a ball mill, and then screened to ensure particle separation; step 4: cobalt is reduced by hydrogen to produce cobalt powder; and step 5: the final WC–Co hardmetal powder

* Fax: +20 2 3370931.
E-mail address: mzawrah@hotmail.com.

0272-8842/$32.00
doi:10.1016/j.ceramint.2005.09.010

is formed by extensive well milling for 24–72 h of WC and Co powder with addition of a lubricant to aid subsequent pressing. Currently, nanostructured WC–Co powder is commercially manufactured through a process called spray conversion processing [9–12]. This process consists of three sequential steps. The first step is to prepare and mix aqueous solutions of the precursor compounds ($CoCl_2$ as Co source and H_2WO_4 and $(NH_3)WO_4$ as W source); the second step is to spray dry the aqueous solution to form a chemically homogeneous powder; and the last step is to thermochemically convert the precursor to the desired nanostructured end-product powder. The thermochemical conversion is conducted in a fluidized bed reactor at 700–900 °C in CO/CO_2 atmosphere. The WC–Co powder produced has a spherical shape, and is hollow and porous with nanograins. In this article, a novel process for preparation of WC–Co nanocomposites in which a polymer as polyacrylonitrile is used as an in situ carbon source will describe. Polyacrylonitrile is a well-known precursor to obtain carbon [13–19].

2. Experimental procedures

Synthesis scheme and steps of WC–Co nanocomposites are given in Fig. 1. Tungstic acid (60 g) was added to obtain 3 L of concentrated ammonium hydroxide in a conical flask (step 1). The mixture was stirred with a magnetic stirrer until nearly all of tungstic acid dissolved. Any trace of undissolved tungstic acid was removed by filtration. The clear solution of ammonium tungstate so obtained had a pH > 12. The excess ammonia in the solution was removed by applying a gentle vacuum until the pH decreased to approximately 8 (step 2). The solution was then transferred to a beaker, and concentrated nitric acid was added under vigorous stirring until the pH of the solution reached approximately 1.6 (step 3). This solution was divided into three parts. 7.26, 4.84 and 2.42 g of $Co(NO_3)_2{\cdot}6H_2O$ were added individually to each part of this solution so that WC–Co containing 15, 10 and 5 wt.% Co could be obtained in the final product. The mixtures were then dried and decomposed on a hot plate to obtain the black mass A. $Co(NO_3)_2{\cdot}6H_2O$ has a dehydration and decomposition temperature of about 55 °C, so drying and decomposition need to be carried out gently and carefully so that no compositional variations occur due to spurting out of the solution.

Acrylonitrile was polymerized to polyacrylonitrile by keeping it with catalyst in 0.1 N nitric acid at 30 °C for 1 h in water bath, then washed and dried (step 4). Three grams of polyacrylonitrile was dissolved in dimethyllformamide (DMF) to obtain a clear solution (step 5); 1.5 g of black mass A was then dispersed in this solution (step 6). The mixture was dried and decomposed on a hot plate and furnace in air at 100–300 °C, to obtain the black mass B (step 7). The black mass could be ground easily into fine powder. Different proportions of the black mass B were then calcined in tube furnace at 800, 900 and 1000 °C in flowing gas mixture of 90% Ar–10% H_2 for 1 h. Another series of tungstate solution containing cobalt and/or iron or manganese or nickel or zinc was prepared by the

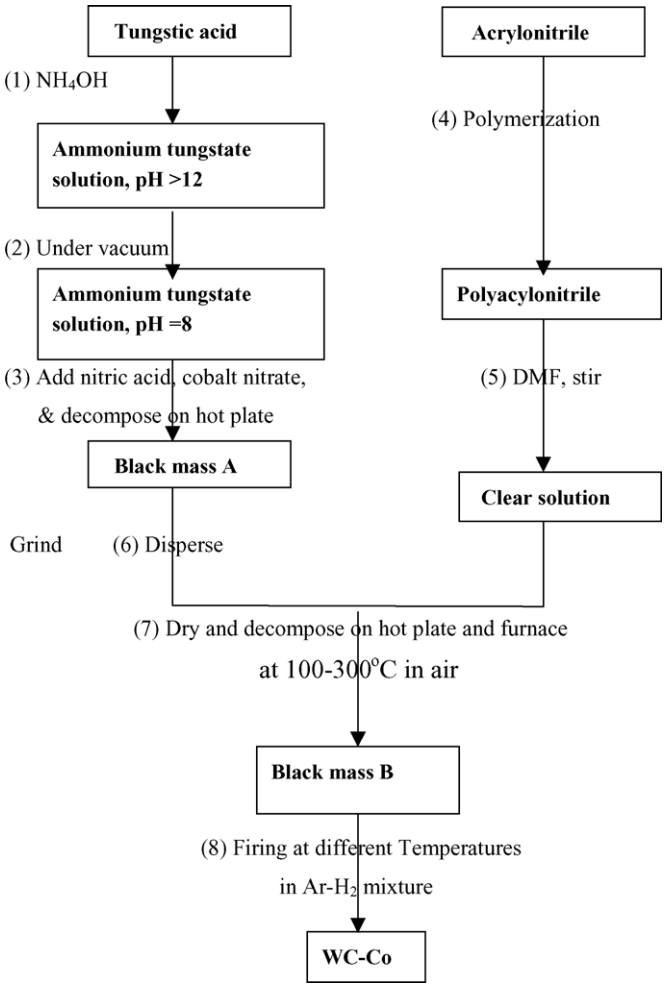

Fig. 1. Synthesis scheme for WC–Co nanocomposites.

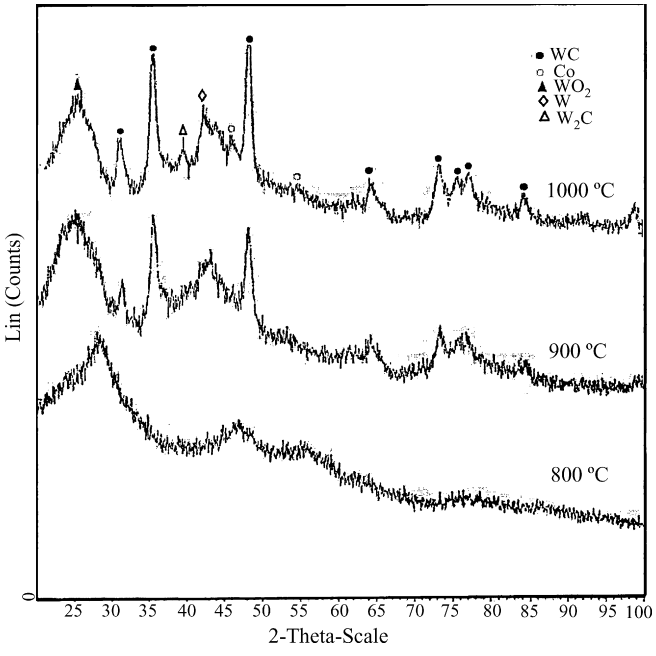

Fig. 2. XRD of WC–Co containing 15 wt.% Co heat treated up to 1000 °C.

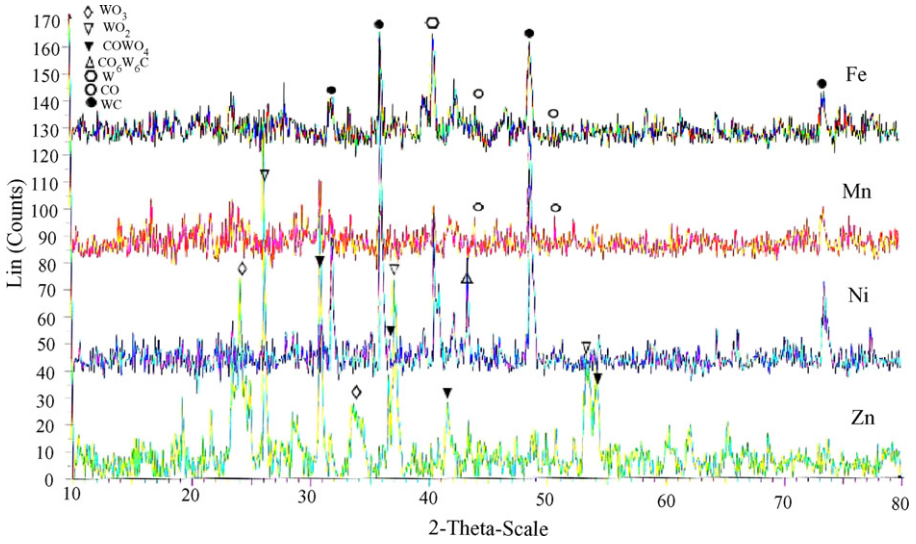

Fig. 3. XRD of WC–Co containing 10 wt.% Co and/or 5 wt.% Fe or Mn or Ni or Zn heat treated at 1000 °C.

same method to produce tungsten carbide containing 10 wt.% cobalt with 5 wt.% of iron or manganese or zinc or nickel. These metals were added in the form of nitrate salt during preparation phase composition and crystallite sizes of the calcined powders were examined by X-ray diffraction. Scherrer formula was used for the determination of the crystallite size from the XRD pattern. The morphology and microstructure of the calcined powders were investigated by transmission electron microscope (TEM) and scanning electron microscope (SEM).

3. Results and discussion

3.1. Phase composition

Characterization of the prepared nanocomposites powders after heat-treatment was investigated by X-ray diffraction (XRD). Fig. 2 shows XRD patterns of heat treated WC–Co nanocomposites containing 15 wt.% cobalt at different firing temperatures. The heat-treated nanocomposite powder at 800 °C is nearly amorphous as shown in Fig. 2 in which the characterizing peaks is very broad. By firing at 900 °C, the peaks broadness decrease, i.e. the crystallinity of the nanocomposite increase. At 1000 °C, sharp and intense peaks characterizing WC–Co nanocomposites powders were obtained as shown in the Figure, i.e. all peaks could be attributed to WC and Co except some peaks characterizing W_2C, W and WO_2 which present in few amount. The results indicate that nearly pure phase of WC–Co nanocomposites can be obtained using polymer precursors as in situ carbon sources after calcination at 1000 °C. XRD patterns of WC–Co nanocomposites containing 5 and 10 wt.% cobalt after heat-treatment at 1000 °C was similar to that obtained with 15 wt.% Co.

XRD patterns of nanocomposites containing 10 wt.% Co with 5 wt.% of Fe or Mn or Zn or Ni are shown in Fig. 3. All samples exhibit characterizing peaks of WC and Co, except the sample-contains Zn which show peaks characterizing oxides of cobalt ($CoWO_4$) and tungsten (WO_2 and WO_3) due to the incomplete reaction, in addition to low intensity peak of WC and Co. The samples containing Fe and Ni show higher

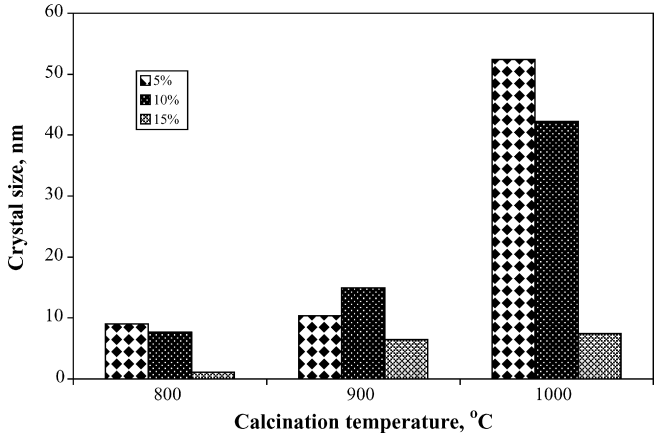

Fig. 4. Effect of heat treatment on crystallite size of WC–Co containing 5, 10 and 15 Co.

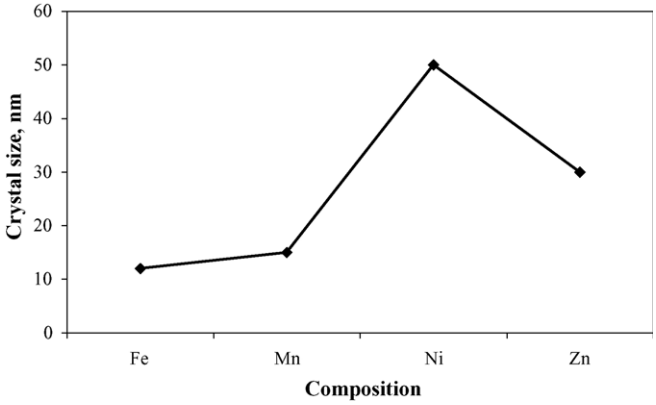

Fig. 5. Crystallite size of WC–10 wt.% Co containing 5 wt.% Fe or Mn or Zn or Ni. Heat-treated at 1000 °C.

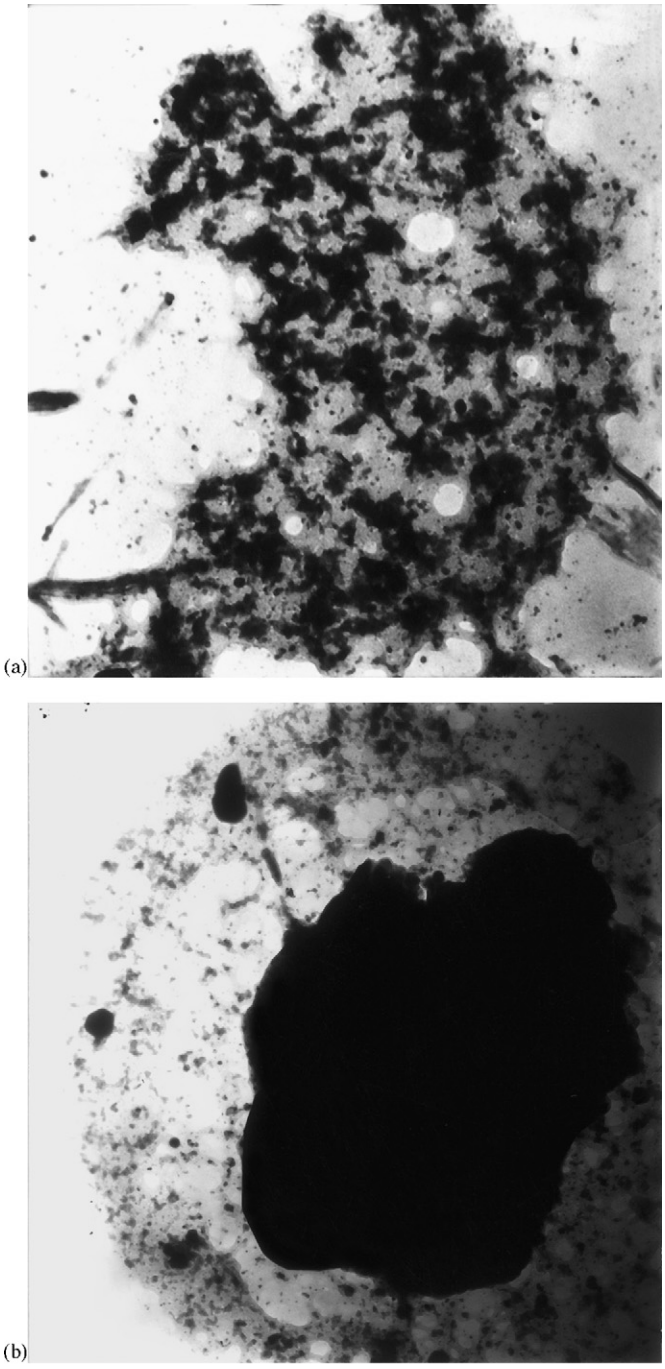

Fig. 6. TEM image of WC–Co containing 15 wt.% Co heat treated up to 1000 °C: (a) ×80,000, (b) ×40,000).

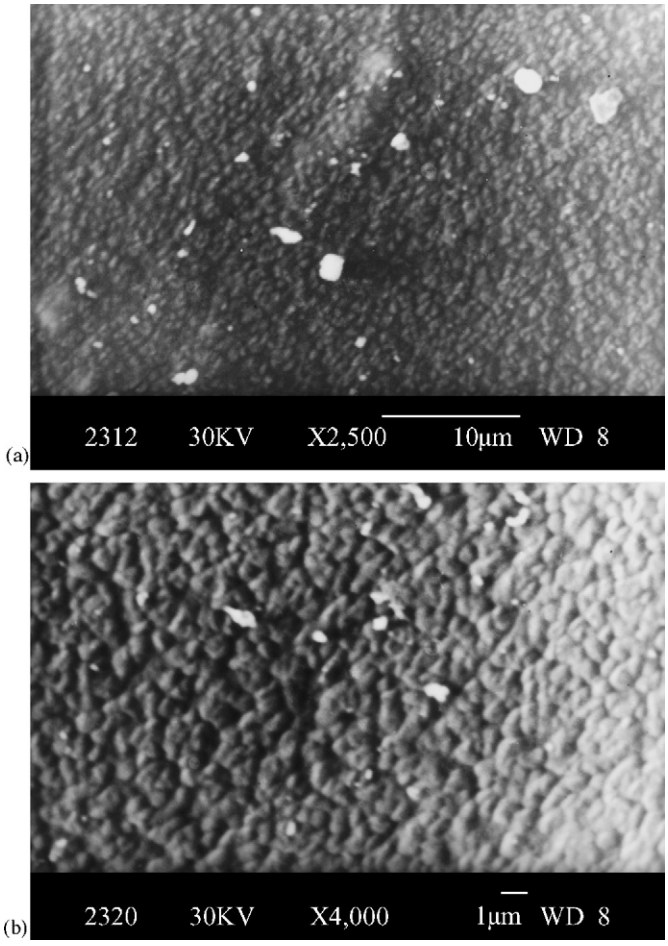

Fig. 7. SEM photomicrograph of WC–Co containing 15 wt.% Co heat treated up to 1000 °C.

intensity characterizing peaks of W, but sample containing Mn exhibits low intensity one. This seams to be due to the present calcination temperature (1000 °C) not enough to form WC by the reaction between W and C, or over degradation of polyacrylonitrile during preparation lead to insufficient carbon. The sample containing Ni exhibits peak characterizing Co_6W_6C. Compounds and/or elements of Fe or Mn or Zn or Ni are also expected to be present in few amounts. However, the firing temperature and time in step 8 as well as the hot plate firing temperature in step 7 play a critical role in obtaining pure phase of WC–Co nanocomposites. Thermal degradation of polyacrylonitrile is complex and occurs over a range of temperatures beginning at around 250 °C [20]. The complexity of the thermal degradation of polyacrylonitrile seems to make the decomposition temperature on the hot plate in step 7 critical as well. The polymer needs to be degraded to the right extent in air at 100–300 °C so that it can latter enhance the WC formation kinetics in step 8 and can provide the right amount of carbon. Over degradation in step 7 may lead to insufficient carbon and formation of Co_6W_6C and or metallic W in the final step. In addition, the higher temperature in step 8 enhances the kinetics of WC formation, but prolonged firing at 900–1000 °C results in the beginning of decomposition of WC. For a given quantity of the black mass, the firing temperature in step 8 should, therefore, be optimized to obtain pure phase products. Difficulties to suppress the formation of Co_6W_6C impurities may also arise from mixing ammonium tungstate and cobalt nitrate solution (step 3), which leads to the formation of $CoWO_4$ precipitate. Once Co_6W_6C is formed, its conversion to WC and Co may be difficult.

Several effects of Co on the formation of WC are found in literatures [21]. First, the reaction sequence has been altered with the addition of Co or CoO [$Co(NO_3)_2$]. For the WO_3

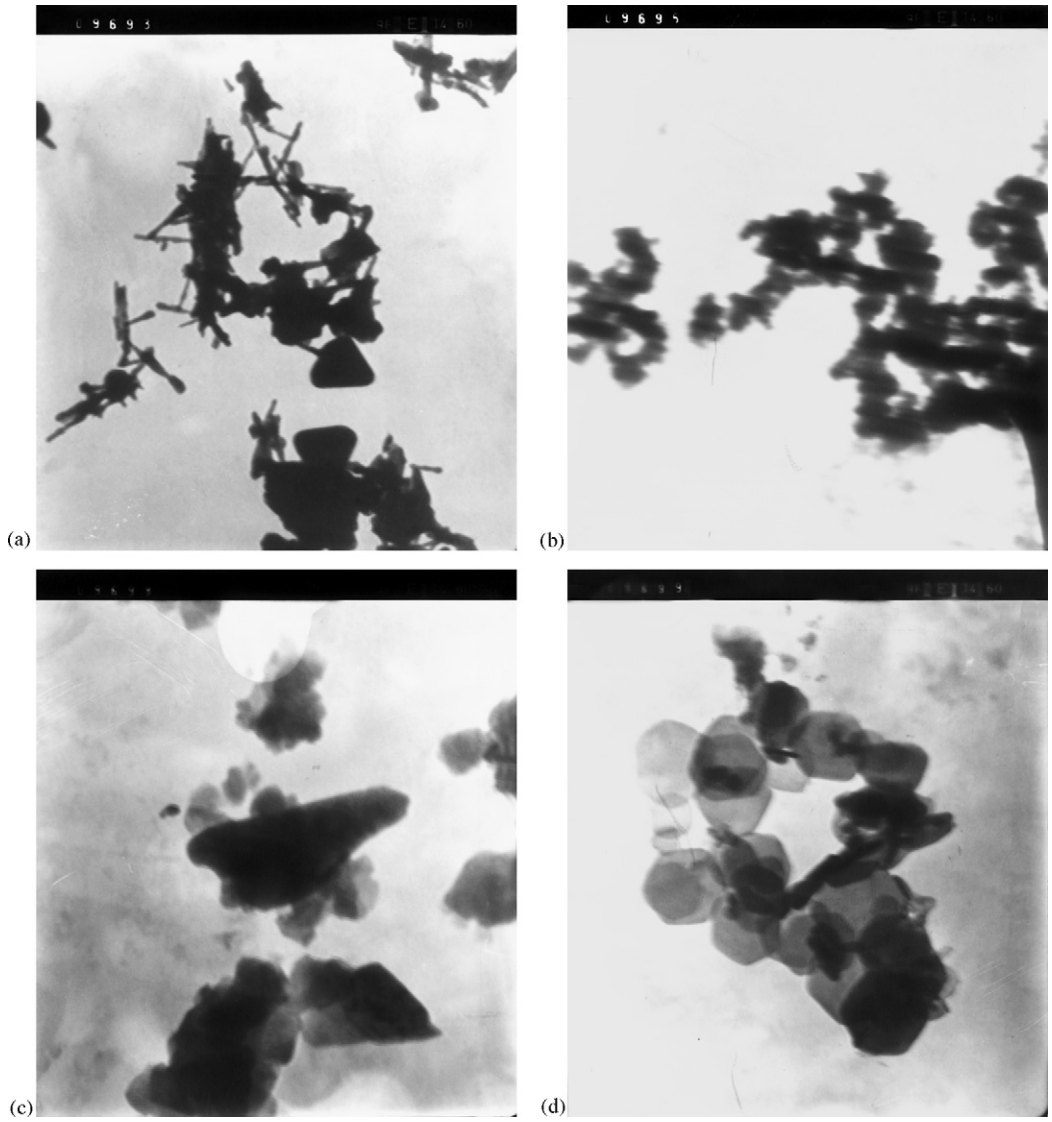

Fig. 8. TEM image of WC-10 wt.% Co containing 5 wt.% Fe (a) or Mn (b) or Ni (c) Zn (d) heat-treated at 1000 °C (×40,000).

(tungestic acid)-plus-carbon system the reaction sequence at 1000 °C is

$$WO_3 \rightarrow W_{18}O_{49} \rightarrow WO_2 \rightarrow W \rightarrow W_2C \rightarrow WC.$$

The reduction sequence found is consistent with the result reported by other investigators [22], and the carburization sequence is also in agreement with the prediction of W–C equilibrium phase diagram [23]. With the addition of CoO to the WO_3-plus-carbon system the reduction sequence of WO_3 remains almost the same; however, the carburization sequence becomes much more complicated with the appearance of several ternary carbides such as Co_6W_6C, CoW_3C (previously known as $Co_3W_9C_4$) and Co_3W_3C. It is found that Co is the one of best catalysis helping the formation of WC. Although there are more phase transformations in the WO_3–CoO–C system than in the WO_3–C system as pointed out previously, the former system in fact has higher WC formation rates. For example, the system WO_3–CoO–C after heating at 1000 °C for 30 min becomes primarily composed of WC, whereas the WO_3–C system with the same processing condition consists mainly W_2C. The enhanced formation of WC in the Co-containing system is most likely to be related to the catalytic behavior of Co. It is well known that Co is one of the best catalysts for the decomposition of CO, which in turn provides active carbon to reduce various oxides and to carburize elemental W and many intermediate compounds (e.g. CO_6W_6C, CoW_3C, Co_3W_3C and W_2C) to form WC. Generally, it should be point out that although the fundamental mechanisms responsible for forming nanostructured WC–Co have not been investigated, a key factor that permits the formation of the nanostructure is the low WC formation temperature; otherwise, grain growth would take place, leading to a loss of nanostructure [24,25].

3.2. Crystallite sizes

Effect of heat treatment up to 1000 °C on the crystallite size of the prepared WC–Co nanocomposites containing 5, 10, and 15 wt.% Co were represented in Fig. 4. Those containing

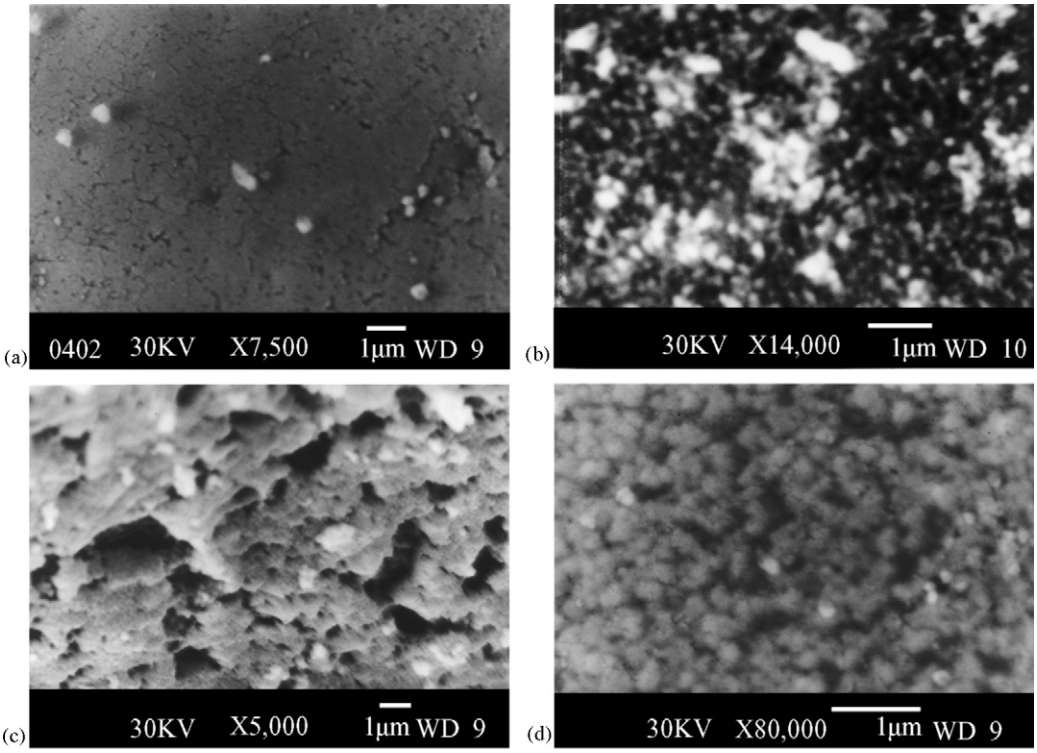

Fig. 9. SEM photomicrograph of WC–10 wt.% Co containing 5 wt.% Fe or Mn or Zn or Ni. Heat-treated at 1000 °C.

10 wt.% Co with 5 wt.% Fe or Mn or Zn or Ni heat treated at 1000 °C are shown in Fig. 5. As appeared from Fig. 4, the crystallite size of WC increases with increasing firing temperature. On the other hand, at the same firing temperature the crystallite size decreases with the increase of cobalt content except that fired at 900 °C which give relatively higher value with 10 wt.% Co. Related to the sample-containing 15 wt.% Co, it appears that the crystallite size of the prepared powders is between 1.1 and 7.4 nm after heat treatment up to 1000 °C, i.e. it still has very low crystallite size even after firing at 1000 °C. All fired samples up to 900 °C have a crystallite size less than 20 nm. The only two samples which give relatively larger crystallite size among all samples are those contain 5 and 10 wt.% cobalt after firing at 1000 °C. On the other side, Fig. 5 exhibits that the crystallite size of WC containing 10 wt.% Co with 5 wt.% Fe or Mn or Ni or Zn calcined at 1000 °C ranged between 12 and 50 nm. The crystallite size of the WC containing Fe, Mn and Zn are 12, 15 and 30 nm, respectively, while the crystallite size of composite sample containing Ni is about 50 nm. The larger crystallite size of the WC containing Ni seems to be due to the complete crystallization of the formed WC phase related to the other composites as indicated from XRD in Fig. 3.

3.3. Morphology and microstructure

The nanocomposite powder morphology and size were tested by TEM and SEM. Figs. 6 and 7 show TEM and SEM of the prepared WC–Co nanocomposite powders containing 15 wt.% Co after heat treated at 1000 °C. TEM micrograph of this sample (Fig. 6) exhibits a particle size range of 200–400 nm with agglomeration of some particle as shown in Fig. 6b. SEM of the same nanocomposite sample is shown in Fig. 7. It shows homogenous microstructure of WC phase (gray phase) with sphere shape particle sized about 500 nm with Co phase (white phase) distributed homogeneously in the microstructure. The nanostructured WC–Co powder is formed from the precursor via a series of decomposition, reduction and carburization. The micron-sized precursor particles are broken into smaller fragments. The fragments shrink further through reduction and carburization reaction and finally nano-sized WC–Co particles in micrometer scale agglomerates are formed.

The morphology and size of prepared WC–10 wt.% Co containing 5 wt.% Fe or Mn or Ni or Zn are shown in Figs. 8 and 9. TEM image (Fig. 8) shows agglomerated and individual particle with different morphology, i.e. spherical, elongated and hexagonal with particle size of about 300–500 nm. The sample containing Zn exhibits hexagonal particles which characterizing the oxides of cobalt and tungsten as confirmed by XRD (Fig. 3). While Fig. 9 shows homogenous microstructure of WC phase (gray phase) with particle size <100 nm in case of WC–Co containing Fe and Mn but >100 nm in case of Zn and Ni. Co and/or Fe or Mn or Ni or Zn phases (white phase) are homogeneously distributed in the microstructure. The as-prepared nanopowder has porous aggregate and spherical morphology. Close examination of the microstructure shows very small WC particles (about 50–100 nm), which appear to be

in different stages of coalescence to form larger particle (200–300 nm).

It is believed that the grain size and grain boundary migration of the WC–Co cements is mainly influenced by firing temperature. The grain boundary mobility can be formulated mathematically to equation [26,27]:

$$B = \frac{D_b}{RT}, \quad (1)$$

$$D_b = D_o \, e\left(\frac{-Q_b}{RT}\right) \quad (2)$$

where B is the mobility of the grain boundary; D_b, grain boundary diffusion; D_o, diffusion constant; Q_b, activation energy of the grain boundary diffusion; R, gas constant and T, firing temperature. From Eqs. (1) and (2), it can be noted that the mobility of the grain boundary B will increase with temperature T. The addition of Co and/or Fe or Mn or Zn or Ni with WC–Co cermets allows chemically activated sintering of nano-WC–Co at lower firing temperature. Therefore, the nanocomposites exhibit much finer microstructure. It is well known that complete substitution of Co binder phase by Fe alloys can be achieved, but at the cost of sintering behavior and lower toughness due to the formation of ferritic bcc structures and an increased risk of forming η-phase double carbides [28–30]. So in the present study the Co binder not completely replaced by Fe or any other additives. According to literature [31,32], Fe–Ni and Fe–Mn systems is a good binding phase materials, so Co–Fe, Co–Mn, Co–Ni and Co–Zn were used in the present work because the similarities between these systems Fe–Ni and Fe–Mn systems.

4. Conclusion

It is concluded that the present chemical method is effective route to synthesize nanocrystalline WC–Co composites. By doping Co and/or Fe or Mn or Zn or Ni in WC–Co nanocomposite, nanocrystalline cemented carbide with inhibited grain growth were obtained. It is found that Co is the one of best catalysis helping the formation of WC. XRD showed peaks characterizing WC and Co in case of WC–15 wt.% Co, but showed addition peaks characterizing some oxides of tungsten and cobalt with W metal in case of WC–10 wt.% Co and/or 5 wt.% Fe of Mn or Zn or Ni. The crystallite size of the prepared WC–15 wt.% Co heat-treated at 1000 °C was in the range of 1.1–7.4 nm, while it was 12–50 nm for WC–Co containing Fe or Mn or Zn or Ni. On the other hand, the particle size was in the range of 200–400 and 300–500 nm, respectively.

References

[1] F. Zhang, J. Shen, J. Sun, The effect of phosphorus additions on densification, grain growth and properties of nanocrystalline WC–Co composites, J. Alloys Compd. 385 (2004) 96–103.

[2] D.H. Jack, Cemented carbide as an engineering material, in: M.M. Schwartz (Ed.), Engineering Application of Ceramic Materials: Source Book, American Society for Metals, Materials Park, OH, 1985, pp. 147–153.

[3] ASM Metals Handbook, 9th ed., vol. 3, Properties and Selection: Stainless Steels, Tool Materials and Special-Purpose Metals; Fabrication of Wrought Stainless Steels, American Society for Metals, Metals Park, Ohio, 1980.

[4] S.W. Yih, C.T. Wang, Tungsten Source, Metallurgy, Properties and Applications, Plenum Press, New York, NY, 1979.

[5] P. Schwarzkopf, R. Kieffer, Refractory Hard Metals, The Macmillan Company, New York, 1953, pp. 138–161.

[6] E.A. Brandles, Hardmetals, in: Smithels Metal Reference Book, sixth ed., Butterworths, Boston, MA, 1983, Chapter 23, p. 4.

[7] S. Komarneni, Nanocomposites, J. Mater. Chem. 2 (12) (1992) 1219.

[8] B. Saruban, Ceramic materials and ceramic matrix composites, in: H. Buhl (Ed.), Advanced Aerospace Materials, Springer-Verlag, New York, 1992, pp. 175–176.

[9] L.E. McCandlish, B.H. Kear, B.K. Kim, Chemical processing of nanophase WC–Co composite powders, Mater. Sci. Technol. 6 (1990) 953–957.

[10] B.H. Kear, L.E. McCandlish, Chemical processing and properties of nanostructured WC–Co materials, Nanostruct. Mater. 3 (1993) 19–30.

[11] L. Gao, B.H. Kear, Low temperature carburization of high surface area tungsten powders, Nanostruct. Mater. 5 (1995) 555–569.

[12] L. Gao, B.H. Kear, Synthesis of nanophase WC powder by a displacement reaction process, Nanostruct. Mater. 9 (1997) 205–208.

[13] T. Yantain Zhu, A. Manthiram, A new route for the synthesis of tungsten carbide–cobalt nanocomposites, J. Am. Ceram. Soc. 77 (10) (1994) 2777–2778.

[14] F.M. Peng, Acrylonitrile polymers, in: H.F. Mark (Ed.), Encyclopedia of Polymer Science and Engineering, vol. 1, Wiley, New York, 1985, p. 426.

[15] D. Seyferth, N. Bryson, D.P. Workman, C.A. Sobon, Preceramic Polymers as 'Reagents' in the Preparation of Ceramics, J. Am. Ceram. Soc. 74 (10) (1991) 2687–2689.

[16] Z. Jiang, W.E. Rhine, Preparation of TiN and TiC from a polymer precursor, Chem. Mater. 3 (6) (1991) 1132–1137.

[17] K. Su, L.G. Sneddon, Polymer-precursor routes to metal borides: synthesis of TiB_2 and ZrB_2, Chem. Mater. 3 (1) (1991) 10–12.

[18] K. Su, M. Nowakowski, D. Bonnell, L.G. Sneddon, Polymer precursor route to TiB_2/TiN nanocomposites, Chem. Mater. 4 (1992) 1141–1144.

[19] R. Corriu, P. Gerbier, C. Guerin, B. Henner, The thermal conversion of poly[(silylene)-diacetylene] metal oxide composites: a new approach to β-SiC-MC ceramics, Angew. Chem. Int. Ed. Engl. 31 (9) (1992) 1195–1197.

[20] F.M. Peng, Acrylonitrile polymer, in: H.F. Mark (Ed.), Encyclopedia of Polymer Science and Engineering, vol. 1, Wiley, New York, 1985, p. 426.

[21] L.L. Shaw, R.-M. Ren, Z.-G. Ban, Z.-G. Yang, A novel process for synthesizing nanostructured WC/Co powders, in: Proceedings of the TMS Fall Meeting, 2000, pp. 75–80.

[22] J. Haber, J. Stoch, L. Ungier, Electron spectroscopic studies of the reduction of WO_3, J. Solid State Chem. 19 (1976) 113–115.

[23] R.V. Sara, Phase equilibria in the tungsten–carbon system, J. Am. Ceram. Soc. 48 (5) (1965) 251–257.

[24] E.K. Storms, Refractory Carbides, Academic Press, New York, 1967, pp. 143–154.

[25] D.H. Jack, Cemented carbide as an engineering material, in: M.M. Schwark (Ed.), Engineering Applications of Ceramic Materials: Source Book, American Society for Metals, Materials Park, OH, 1985, pp. 147–153.

[26] S. Yan, W. Xin, Y. Xuegang, J. Chin. Ceram. Soc. 31 (3) (2003) 278–282.

[27] T. Yamaoto, Y. Ikuhara, T. Sakuma, High resolution transmission electron microscope study in VC-doped WC–Co compound, Sci. Technol. Adv. Mater. 1 (2000) 97–104.

[28] O. Kubesschewski, Cb. Alcock, P.J. Spencer, Materials Thermo chemistry, sixth ed., Pergamon, New York, NY, 1993.

[29] T. Farooq, T.J. Davies, Preparation of some new tungsten carbide hard metals, Powder Metall. Int. 22 (1990) 12–16.

[30] B.H. Kear, G. Skandan, R.K. Sadangi, Factors controlling decarburization in HVOF sprayed nano-WC–Co hardcoatings, Scripta Mater. 44 (2001) 1703–1707.

[31] T. Farooq, T.J. Daves, Tungsten carbide hard metals cemented with ferroalloys, Int. J. Powder Metall. 27 (1991) 347–355.

[32] C. Hanyaloglu, B. Aksakal, J.D. Bolton, Production and indentation of WC/Fe–Mn as an alternative to cobalt-bonded hardmetals, Mater. Characterization 47 (2001) 315–322.